Scientia Iranica B (2022) 29(4), 1795–1805

Sharif University of Technology
Scientia Iranica
Transactions B: Mechanical Engineering
http://scientiairanica.sharif.edu

Optimization of plasma enhanced chemical vapor deposition process parameters for hardness improvement of diamond-like carbon coatings

K. Kalita[a] and R. Kumar Ghadai[b,*]

a. *Department of Mechanical Engineering, Vel Tech Rangarajan Dr. Sagunthala R&D Institute of Science and Technology, Avadi, Tamil Nadu, India 600062.*
b. *Department of Mechanical Engineering, Sikkim Manipal Institute of Technology, Sikkim Manipal University, Majhitar, Sikkim, India 737136.*

Received 25 September 2020; received in revised form 20 August 2021; accepted 25 April 2022

KEYWORDS
Metaheuristics;
DLC;
Metamodel;
PSO;
Regression;
Thin film;
PECVD.

Abstract. Recently, there has been a surge in the use of metaheuristic algorithms to design materials with optimum performance. In this paper, the RPSOLC (Repulsive Particle Swarm Optimization with Local search and Chaotic perturbation) metaheuristic algorithm was used to design Diamond-Like Carbon (DLC) thin films with improved hardness. Based on the Box-Behnken design, 15 independent DLC deposition experiments are performed in a PECVD (Plasma-Enhanced Chemical Vapor Deposition) setup by varying the CH_4-Argon flow rate, hydrogen flow rate, and deposition temperature. The nano-hardness of the DLCs is evaluated using nano-indention tests. The hardness is then expressed as the function of the three process parameters using a polynomial regression metamodel. Finally, using RPSOLC, the metamodel is optimized and compared to the optimal predictions of a traditional Genetic Algorithm (GA). It is seen that RPSOLC has faster convergence and is more reliable than the GA. In general, a high H_2 flow rate along with a low CH_4-Ar flow rate and high temperature is found to be beneficial in improving the hardness.

1. Introduction

Other than graphite and diamond, Diamond-Like Carbon (DLC) is a significant material in the carbon group [1]. DLC is basically a hybrid form of carbon that holds both graphite-like sp2 bonds and diamond-like sp3 bonds [2]. Apart from its unique structures DLC coatings possess superb tribological, optical, mechanical, and electronic properties which led them to the significant industrial application [3]. DLC has the properties of both graphite and diamond because it contains a combination of sp2 and sp3 bonds [4]. The good tribological and mechanical properties of DLC are basically due to the presence of sp3 hybridized carbon whereas, electrical and electronic properties are due to the sp2 hybridized carbon [5]. DLC coating is also used for making magnetic storage discs, micro-electromechanical devices, bio-implants, engine parts, etc. [6]. Vapour deposition techniques are generally used for the deposition of thin-film coatings and out of all the vapour deposition techniques Chemical Vapour Deposition technique (CVD) is the most widely used

*. *Corresponding author. Tel.: +91-9038109904*
E-mail addresses: kanakkalita02@gmail.com (K. Kalita); ranjankumarbls@gmail.com (R. Kumar Ghadai)

doi: 10.24200/sci.2022.56869.4952

synthesis method for the DLC coating. Other than DLC coatings, the CVD process is also used for the synthesis of different metal alloy compounds, such as nitrides, carbides, and oxides [7,8]. CVD techniques are seen to be a viable choice for thin-film coating deposition since they create a variety of products with good wear resistance, hardness (H), coefficient of friction (F), young modulus (E), and oxidation resistance. Out of all the CVD processes, Plasma-Enhanced Chemical Vapor Deposition (PECVD) is the most suitable method for the deposition of DLC thin-film coating due to the low deposition temperature [9]. The properties of DLC coating can be affected by PECVD process parameters such as gas flow rate, deposition temperature, duty cycle, gas composition, and power supply [7,9]. The main problem for the researchers is to determine the combination of deposition parameters to get the optimal response parameter. Various optimization techniques such as artificial neural networks, Genetic Algorithms (GA), grey relational analysis, adaptive neuro-fuzzy inference system, and others could be used to optimize the PECVD process parameters in order to achieve the optimum output. To optimize the properties of Zr-DLC coatings, Yang and Huang adopted a grey-fuzzy and Taguchi technique [10]. Using the Taguchi technique, Singh and Jatti predicted the optimal combination of process parameters to maximize hardness, including deposition pressure, bias frequency, bias voltage, and gas composition [11]. Ghadai et al. used the GA technique to optimize the process parameters for Atmospheric Pressure Chemical Vapour Deposition (APCVD) to improve mechanical properties like H and E [12].

From the literature survey, it is seen that most authors so far have relied on Multi-Criteria Decision-Making (MCDM) tools to find the optimal process parameter combination. However, because MCDM techniques lack a powerful full domain search, their predictions are frequently subpar when compared with metaheuristic search-based optimal predictions. This paper makes three primary contributions:

1. While most literature has focused on CVD techniques, DLCs used in this research are deposited using PECVD;
2. Experimental nano-hardness is obtained for DLCs which would serve as a benchmark for future studies;
3. A novel memetic PSO called RPSOLC is used for the optimal design of DLCs.

2. Materials and methods

2.1. Response surface metamodel

In this research, a second-order polynomial model of the following form is considered as the response surface metamodel [13,14]:

$$\hat{y} = \beta_0 + \sum_{i=1}^{k} \beta_i x_i + \sum_{i=1}^{k} \sum_{j>i}^{k} \beta_{ij} x_i x_j + \sum_{i=1}^{k} \beta_{ii} x_i^2 + \varepsilon, \quad (1)$$

where $\hat{y}$ is the metamodel for the hardness of the DLC coating, x_i is the process parameters, β_0, β_i, β_{ij}, and β_{ii} are the unknown regression coefficients to be determined by fitting the training data to Eq. (1) such that the sum of squares of the residuals (SS_R) is minimized. The SS_R is calculated as follows:

$$SS_R = \sum_{i=1}^{n} (y_i - \hat{y}_i)^2, \quad (2)$$

where y_i is the experimental training data point.

The experimental design for the training data points is decided as per Box-Behnken Design (BBD). For each process parameter, BBD has three levels (-1, 0, and $+1$). Table 1 shows the coded and uncoded BBD designs used in this study. The total training data points as per BBD is determined using the following relation:

$$n = 2k(k-1) + c_o, \quad (3)$$

where n is the number of training data points, k is the number of process parameters and c_o is the number of repetitions of the central point.

2.2. Experimental procedure

In the present research, PECVD is used for the synthesis of DLC coatings over P-type silicon (Si) substrate. Initially, the Si substrate was cleaned for 4 minutes in a 2% HF solution to remove the oxide layer. After the removal of the oxide layer, the substrates are ultrasonically cleaned for 10 minutes by using deionizing water. CH_4-Argon (Ar) flow rate, Hydrogen (H_2) flow rate, and deposition temperature (T_d) are considered deposition parameters for the optimization of hardness as shown in Table 1. Surface roughness (Ra) and particle size of PECVD deposited DLC coatings were measured by using the AFM (model: INNOVA SPM). In the AFM the precise topographic images of the films are taken by scanning the surface with a nanometre-scale probe (vertical $\sim$ 0.1 nm, lateral resolution $\sim$ 1 nm). For the films, the surface roughness, as well as maximum and average particle size, were evaluated at a 10 μm level. The nano-indentations are performed using a CSM instruments nano-hardness tester (NHTX-55–0019). For indentation, a Berkovich diamond indenting tip (B-I 93) with a tip radius of 100 nm is used. A constant indentation load of 20 mN is considered at three different locations and the indentations over the sample and their average number are reported. During the indentation, the rate

Table 1. Box-Behnken DOE and experimental values.

Std. Ord.	Coded process parameters			Un-coded process parameters			Output hardness (GPa)
	CH_4-Argon flow rate	H_2 flow rate	Deposition temperature	CH_4-Argon flow rate	H_2 flow rate	Deposition temperature	
1	−1	−1	0	0.5	20	100	14.40
2	1	−1	0	2	20	100	15.20
3	−1	1	0	0.5	40	100	15.50
4	1	1	0	2	40	100	17.34
5	−1	0	−1	0.5	30	80	11.28
6	1	0	−1	2	30	80	12.92
7	−1	0	1	0.5	30	120	19.20
8	1	0	1	2	30	120	16.42
9	0	−1	−1	1	20	80	13.20
10	0	1	−1	1	40	80	12.20
11	0	−1	1	1	20	120	14.60
12	0	1	1	1	40	120	21.56
13	0	0	0	1	30	100	15.56
14	0	0	0	1	30	100	16.90
15	0	0	0	1	30	100	16.80

of loading-unloading was 10 mN/min and at the peak load of 20 mN, the indenter was paused for 10 sec. The Oliver–Pharr method [15] is used for hardness calculation. The indentation hardness is calculated by using the following equation:

$$H = \frac{P_{\max}}{A}, \tag{4}$$

where $P_{\max}$ is the maximum load applied over the work piece and A is the contact area of the tip of the indenter over the coating. In [16], a detailed analysis has been done over the nanoindentation phenomenon by considering different spherical indenter tips.

2.3. Repulsive Particle Swarm Optimization with Local search and Chaotic perturbation (RPSOLC)

Particle Swarm Optimization (PSO) is a widely used metaheuristic in various fields of engineering [17–20]. In this research, a novel memetic version of PSO [21] called RPSOLC (Repulsive Particle Swarm Optimization with Local search and Chaotic perturbation) [22] is used. Any typical PSO algorithm starts by generating a set of random solutions (called particles) in the design space. In PSO terminology, this set of solutions is collectively called the swarm [23,24]. Each particle within the swarm is aware of its personal best position called the $pBest$. The particles in the swarm are also aware of the $gBest$, which is the overall best position (or solution) found so far. All particles try to move towards the $gBest$ position by using the following two rules to update their velocity and position:

$$v_{t+1} = \omega.v_t + c_1.r_1.(pBest - x_t) + c_2.r_2.(gBest - x_t), \tag{5}$$

$$x_{t+1} = x_t + v_{t+1}, \tag{6}$$

where v_t and v_{t+1} are the velocity in the current and the next generation respectively. Similarly, x_t and x_{t+1} are the positions of the particle in the current and the next generation respectively. r_1 and r_2 are two random numbers between 0 to 1. c_1 and c_2 are called the cognitive and social parameters. The effect of the velocity of the previous generation on the velocity of the current generation is controlled by the inertia weight ω.

Despite the fact that PSO is a stochastic technique, Standard Particle Swarm Optimization (SPSO) for complicated problems has a tendency to get stuck in local optima [25,26]. To counter this issue, Urfalioglu [27] proposed the Repulsive Particle Swarm Optimization (RPSO) in which the particles update their velocity using the relation below:

$$v_{t+1} = \omega.v_t + \alpha.r_1.(pBest - x_t) + \omega.\beta.r_2.(\widetilde{pBest} - x_t) + \omega.\gamma.r_3.v_t^r, \tag{7}$$

where α, β, γ are constants. The term $\alpha.r_1.(\widetilde{pBest} - x_t)$

leads any particle towards its self-best position. The term $\omega.\beta.r_2.(\widetilde{pBest} - x_t)$ leads the particle away from a randomly chosen particle from the swarm. The term $\omega.\gamma.r_3.v_t^r$ is responsible for the exploration of new search regions.

In this paper, the traditional RPSO is further upgraded by incorporating the memetic attributes suggested by Santos et al. [28,29]. Each particle is endowed with the ability to conduct a local search by visiting its surroundings by using a parameter called *nstep*. The visit is independent of the gradient in any direction and thus is free from bias. If any particle is seen to be trapped in one position even after a pre-defined number of multiple generations a small random disturbance in its velocity (called the chaotic perturbation) is inserted.

$$x_{t+1} = x_t + v_{t+1}.(1 + r_{chaos}), \tag{8}$$

where r_{chaos} is the chaotic perturbation. This helps the RPSOLC algorithm avoid getting trapped in local optima pits. The current RPSOLC pseudocode can be found in the authors earlier work [30].

It should be noted that the stochasticity of SPSO is due to r_1 and r_2. Similarly, RPSO is dependent on r_1, r_2, and r_3 for stochastic search. Moreover, r_1, r_2, and r_3 should be vectors of random values. If they are scalers, only linear combinations of the initial particle positions will be searched. Thus, it may be argued that to some extent r_1, r_2, and r_3 aid the algorithm in avoiding local optima by introducing stochasticity. The r_{chaos} is a much smaller perturbation as compared to r_1, r_2, and r_3 and is applied occasionally, if the algorithm 'feels' it is trapped in local optima.

3. Results and discussion

3.1. Metamodel building and evaluation

A second-order polynomial metamodel describing the coating nano-hardness as a function of the CH_4-Ar flow rate, H_2 flow rate, and deposition temperature (T_d) is developed as shown in Eq. (9):

$$\begin{aligned} H = (&-3.1282 + 9.9245x_1 - 0.7883x_2 \\ &+0.3379x_3 + 0.0185x_1x_2 - 0.0681x_1x_3 \\ &+0.0100x_2x_3 - 1.3700x_1^2 - 0.0019x_2^2 \\ &-0.0021x_3^2), \end{aligned} \tag{9}$$

where x_1, x_2, and x_3 represent CH_4-Ar flow rate, H_2 flow rate, and deposition temperature respectively.

The predicted nano-hardness by the metamodel and the experimental nano-harness of the coatings are compared in Figure 1. It is seen that the data points in Figure 1 are very close to the diagonal line which indicates a very high accuracy in the prediction of the metamodel. The analysis of the residuals with respect to the predicted nano-hardness in Figure 2 shows that the residuals are arbitrarily distributed in the graph. The lack of any visible pattern in the residuals of the metamodel indicates that the data do not have any ties. Furthermore, this shows that the measuring resolution is adequate. Figure 2 further shows that the residuals arbitrarily take on both negative and positive values, indicating that the metamodel is not biased and that any arbitrary combination of process parameters has an equal chance of being underpredicted or overpredicted. Since the normality of residuals is an important construct in many statistical analyses, a normality test is carried out for the metamodel residuals. From Figure 3 it is seen that the residuals follow a normal curve since they are very close to the reference line.

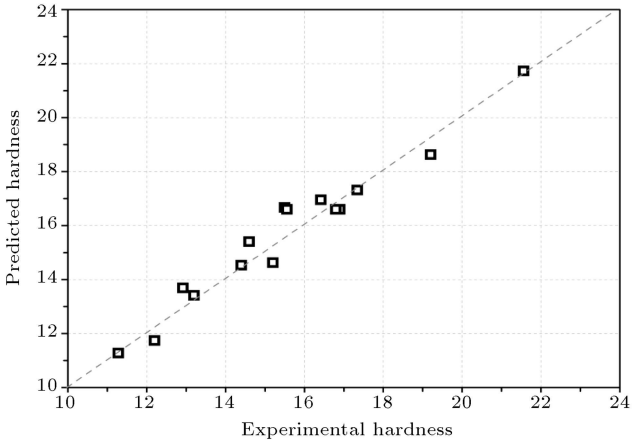

Figure 1. Predicted response versus experimental response.

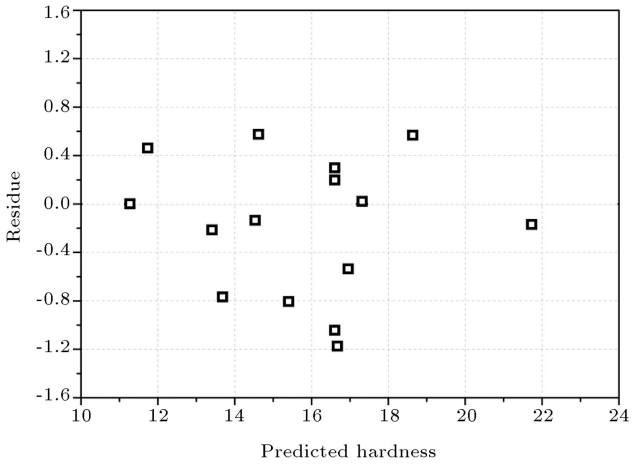

Figure 2. Residuals versus the predicted response.

3.2. Parametric study of the process parameters

The developed metamodel is used in this section to understand the effect of the deposition process param-

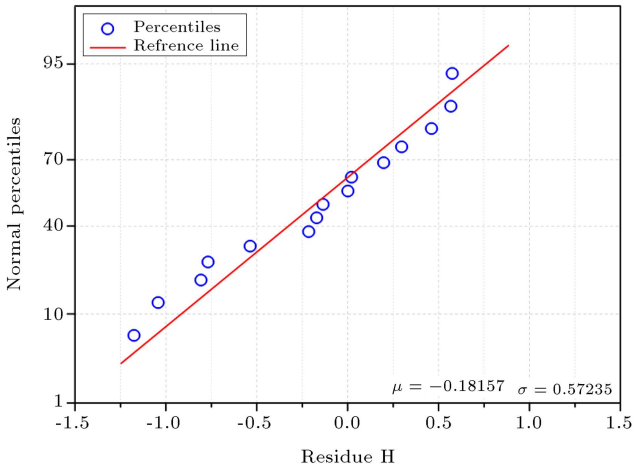

Figure 3. Normal probability plot for the metamodel.

eters on the nano-hardness of the coatings. Figure 4 shows the effect of the CH_4-Ar flow rate and the H_2 flow rate on the nano-hardness at three different levels of deposition temperature. It is seen that for all other parameters kept constant, in general, the hardness of the coatings will increase if the deposition temperature is increased. However, from Figure 4 it is seen that at low deposition temperature the increase in H_2 flow rate reduces the coating hardness which is opposite to the trend shown in mid-level and high temperatures. At mid-level and high temperatures, the increase in H_2 flow rate is accompanied by increased hardness. Overall, from all the three subplots of Figure 4, it is observed that a high temperature with a high H_2 flow rate and low CH_4-Ar flow rate is most suitable for increasing the coating hardness.

Similarly, the effect of CH_4-Ar flow rate and deposition temperature on the nano-hardness of the DLCs at different H_2 flow rates is studied in Figure 5. Typically, the hardness is seen to be positively impacted by the increased H_2 flow rates. Here, unlike Figure 4, all the three sublots show similar trends i.e., the coating nano-hardness increases with the increase in deposition temperatures. However, the trend of the hardness with respect to the CH_4-Ar flow rate at low deposition temperatures is contrary to that at high deposition temperatures. While at high deposition temperatures low CH_4-Ar flow rates are desirable, the performance of the coatings in terms of hardness is

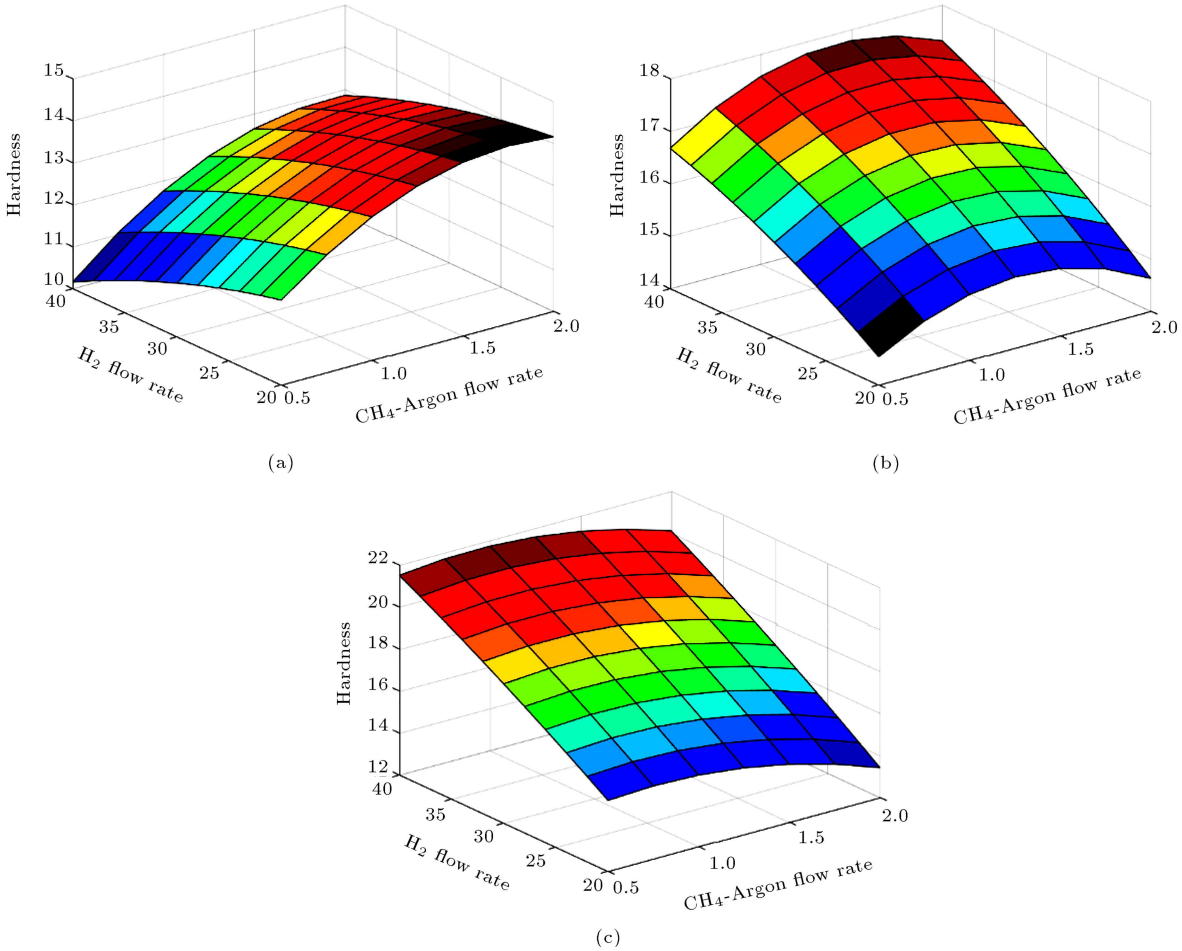

Figure 4. Effect of H_2 flow rate and CH_4-Argon flow rate on coating hardness at (a) $T = 80°C$, (b) $T = 100°C$, and (c) $T = 120°C$.

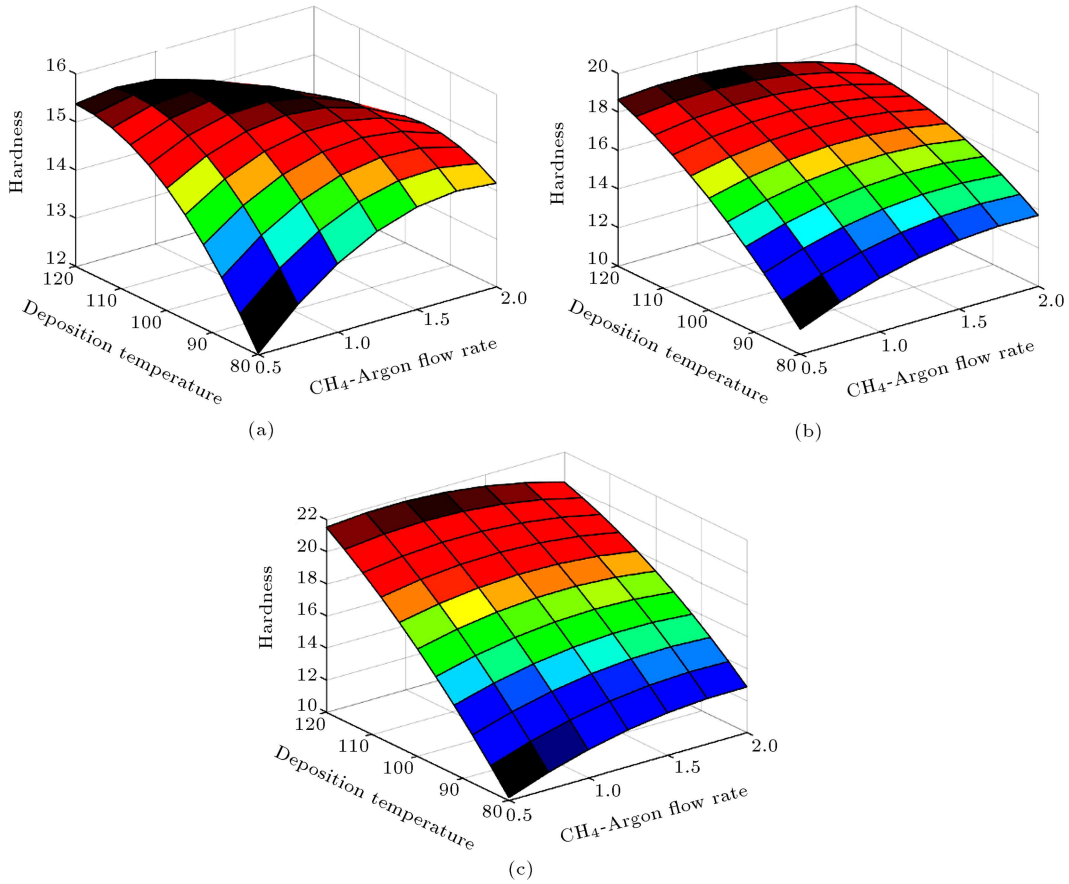

Figure 5. Effect of deposition temperature and CH_4-Argon flow rate on coating hardness at different H_2 flow rate: (a) 20 sccm, (b) 30 sccm, and (c) 40 sccm.

better at high CH_4-Ar flow rates when low deposition temperatures are considered. Figure 6 shows the combined effect of deposition temperature and H_2 flow rate at different CH_4-Ar flow rates.

3.3. Optimization study

The hardness exhibits a non-linear relationship with the CH_4-Ar flow rate, H_2 flow rate, and deposition temperature (T_d), as shown by the parametric investigation of the process parameters in the previous section. Thus, it is necessary to use a metaheuristic-based search to find the optimal parameter settings to maximize the nano-hardness. The various tuning parameters used for the RPSOLC algorithm are: $\omega = 0.5$, $\alpha = 0.5$, $\beta = 0.5$, $\gamma = 0.005$, swarm size = 50, $nstep = 10$, iteration limit = $100.r_1, r_2, r_3$ are three random numbers ranging from 0 to 1. For the GA algorithm the following tuning parameter values are used: population size = 500, generation limit = 100, crossover probability = 90%, mutation probability = 5%, length of chromosomes = 12 bit. Binary encoding is used for the GA and one-point crossover is used.

Figure 7 shows the improvement of the fitness function (i.e., nano-hardness) as the generations progress for a typical trial. It is seen that RPSOLC has a faster rate of convergence as compared to the traditional GA. However, in this trial, both the metaheuristic algorithms- RPSOLC and GA are seen to converge to the same final optimum.

To further understand the optimum prediction capability of the algorithms, the 50,000 function evaluations of the algorithms for a typical trial are analyzed in Figure 8. The box plot of the GA has a larger spread as compared to the RPSOLC plot. Also, the fitting of the evaluated function data points to a normal curve shows that the GA follows a more normal trend indicating that the maximum evaluated points in the GA trial are around its mean value and thus would take longer to converge. On the other hand, for RPSOLC the data points are seen to form a large cluster at the top with a long and narrow tail in the bottom portion. This indicates that on average the RPSOLC would have higher fitness than the GA, which is also indicated by the relative higher position of the mean value of the RPSOLC evaluations in the Box plots.

Figure 9 shows that GA could only reach the maxima in three of the 50 independent trials, whereas the RPSOLC predicted it in all the 50 trials. This indicates that the RPSOLC is more reliable as compared to the traditional GA. Computer codes for GA and

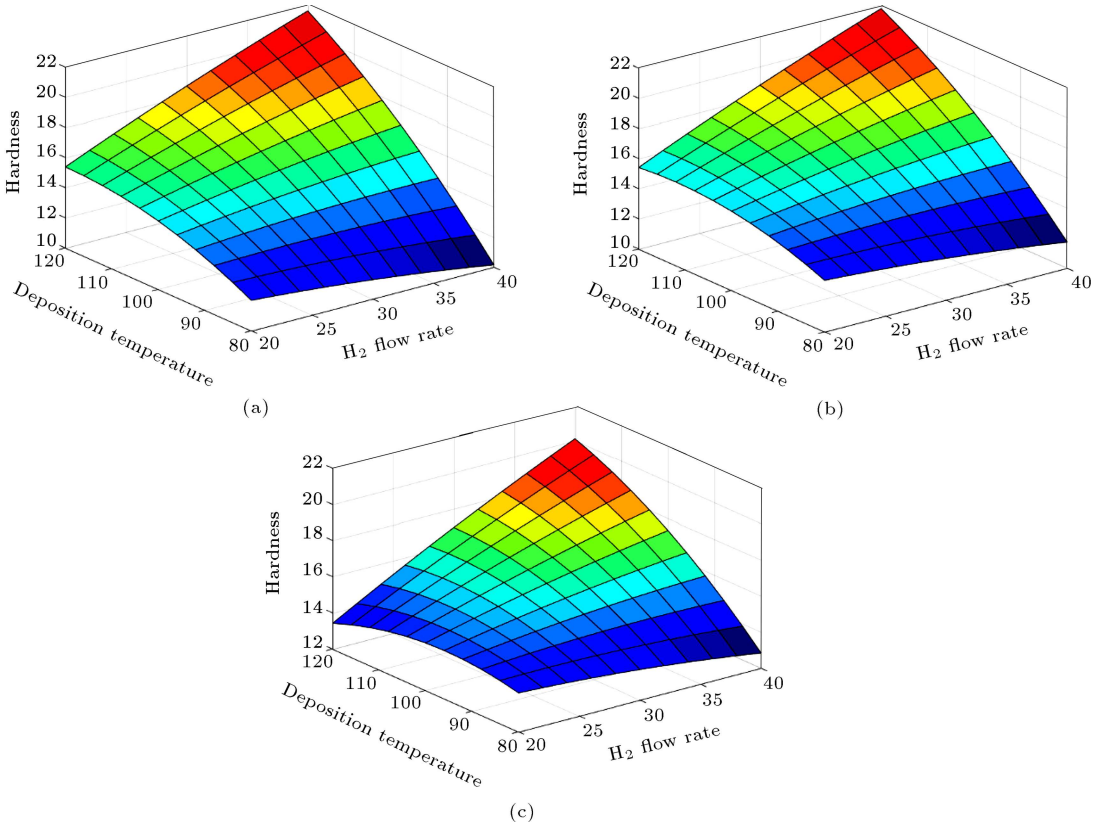

Figure 6. Effect of deposition temperature and H_2 flow rate on coating hardness at different CH_4-Argon flow rate: (a) 0.5 sccm, (b) 1 sccm, and (c) 2 sccm.

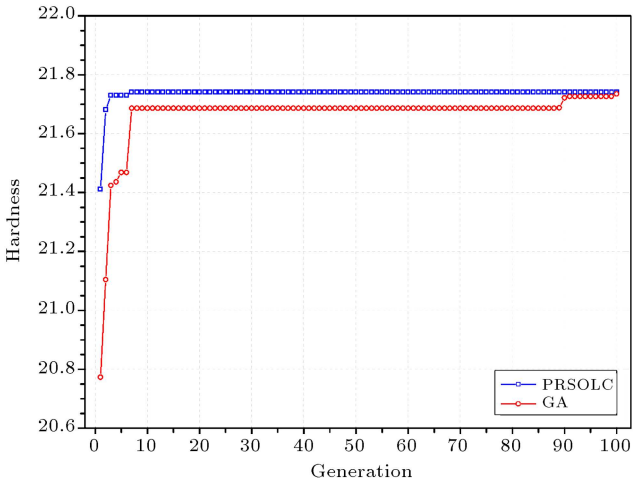

Figure 7. Convergence of the algorithms across generations.

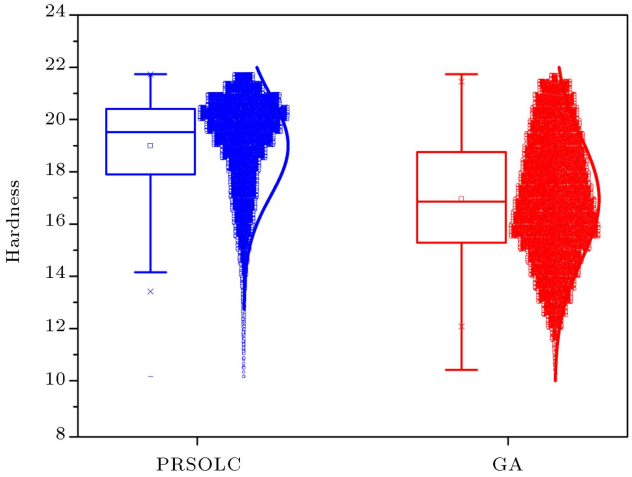

Figure 8. Box plot depicting spread of 50,000 functions evaluations for each algorithm.

RPSOLC are developed in Fortran language and the simulations are carried out on a Dell Inspiron 15-3567 series windows system with Intel(R) Core TM i7-7500U CPU @2.70 GHz, Clock Speed 2.9 Ghz, L2 Cache Size 512 and 8 GB ram. For 50 independent trials, the total runtime for GA was approximately 845 seconds. The RPSOLC is seen to have approximately 15% less runtime as compared to the GA. Thus, it is seen that the RPSOLC is faster compared to the GA.

3.4. Analysis of the experimental results and optimum results

The optimal process parameter combination and the maximized hardness predicted by the RPSOLC and the GA are shown in Table 2. Figure 10 shows the loading-unloading curve of the optimal point. Similarly, the loading-unloading curve of experiments no. 2, 7, and 12 is shown in Figure 11. From the figure, it has been observed that for a fixed load of 20 mN, the depth of

Table 2. Optimum deposition process parameters predicted by RPSOLC and GA.

Optimum predicted parameters			Hardness (GPa)
CH_4-Ar flow rate (sccm)	H_2 flow rate (sccm)	T_d (°C)	Predicted
0.9	40	120	21.74

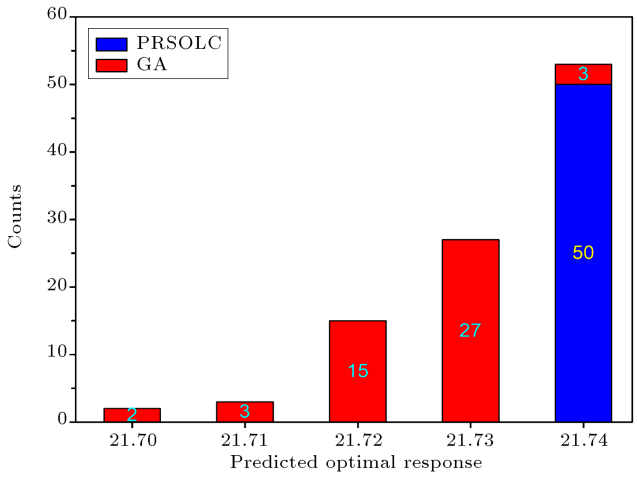

Figure 9. Values of optimum predicted by the algorithms in 50 independent trials.

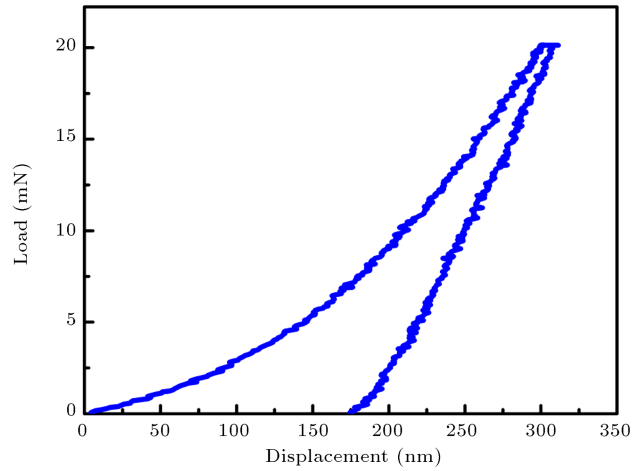

Figure 10. Loading-unloading curve of optimal point.

indentation of the sample at experiment no. 2 is larger as compared to experiments no. 7, 12, and optimum point which revealed that the sample at experiment no. 2 has low hardness. The hardness of the sample increases with higher deposition temperature and H_2 flow rate, as seen in Tables 1 and 2. This could be because, at higher deposition temperatures and H_2 flow rates, more sp3 bonds form within the film [31,32]. Figure 12 shows the 3D and 2D AFM images of the samples at the optimal point. Similarly, Figures 13 and 14 show the AFM images for experiment no. 7 and experiment no. 12 respectively. For each sample, the maximum particle size, as well as the surface roughness

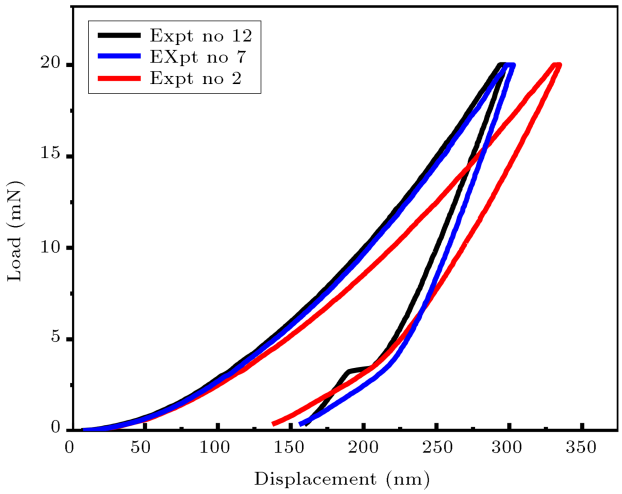

Figure 11. Loading-unloading curve of experiments no. 2, 7, and 12.

of the coating were evaluated at a 10 μm level. The surface roughness of the sample at the optimal point, experiment no. 7 and experiment no. 12 are found to be 28.6 nm, 18.2 nm, and 22.3 nm respectively. At high temperature and high H_2 flow rate agglomerated particles are observed over the surface of the coatings [33]. The maximum particle size of coating at the optimal point, experiment no. 7 and experiment no. 12 are observed to be 14.3 nm, 2.2 nm, and 4.4 nm respectively. From the AFM results, it is noticed that the particle size of the coating is maximum at a higher H_2 flow rate, CH_4-Ar flow rate, and deposition temperature.

4. Conclusion

In this paper, Diamond-Like Carbon (DLCs) were designed for better hardness by using an optimal combination of CH_4-Argon flow rate, hydrogen flow rate, and deposition temperature. The optimal process parameters were searched using an RPSOLC algorithm. The Repulsive Particle Swarm Optimization with Local search and Chaotic perturbation (RPSOLC) demonstrated faster convergence as compared to a traditional Genetic Algorithm (GA), which can be attributed to its local search capability. The results of the repeated trials also showed higher reliability of the RPSOLC compared to the GA. For all the 50 trials, the RPSOLC was successfully able to locate the maxima whereas

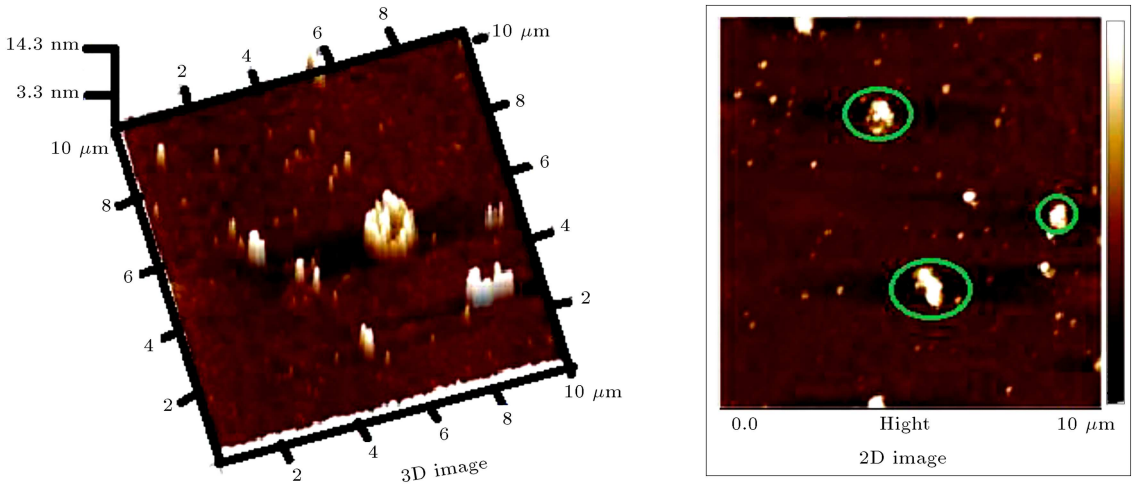

Figure 12. AFM images of optimum point.

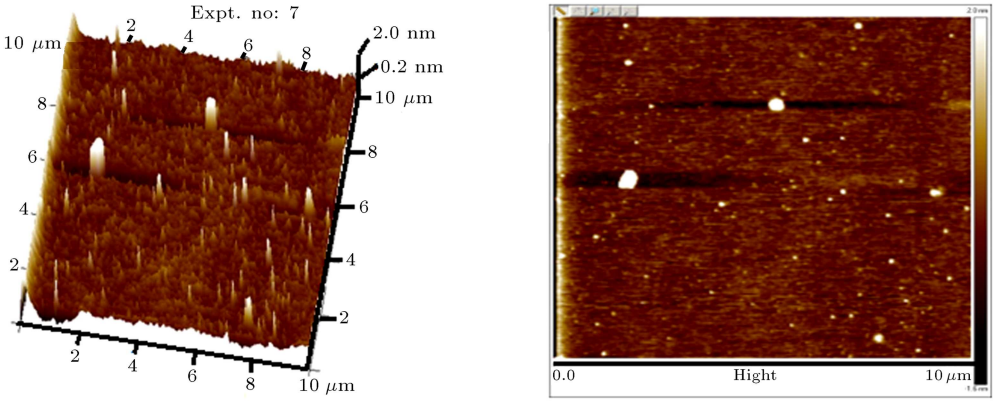

Figure 13. AFM images of experiment no. 7.

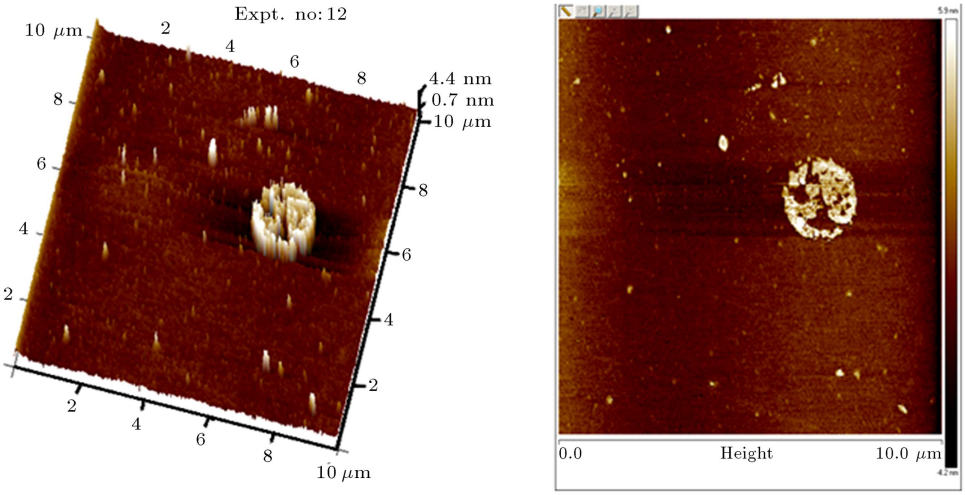

Figure 14. AFM images of experiment no. 12.

the GA predicted sub-optimal solutions in 47 trials. This success of RPSOLC can be attributed to the chaotic perturbation that helped it avoid the pit of local optima. The optimal process parameters (CH_4-Ar flow rate, H_2 flow rate, and T_d) were recorded as 0.9 sccm, 40 sccm, and 120 °C respectively. Thus, it can be concluded that the RPSOLC combined with polynomial metamodels can be used as a viable and efficient tool to fine-tune the design process of sophisticated materials like thin-film coatings.

Nomenclature

APCVD	Atmospheric Pressure Chemical Vapour Deposition
BBD	Box-Behnken Design
CVD	Chemical Vapour Deposition
DLC	Diamond-Like Carbon
GA	Genetic Algorithm
MCDM	Multi Criteria Decision Making
PECVD	Plasma Enhanced Chemical Vapor Deposition
PSO	Particle Swarm Optimization
RPSOLC	Repulsive Particle Swarm Optimization with Local search and Chaotic perturbation
SPSO	Standard Particle Swarm Optimization

References

1. Dwivedi, N., Kumar, S., and Malik, H.K. "Nanostructured titanium/diamond-like carbon multilayer films: deposition, characterization, and applications", *ACS Applied Materials & Interfaces*, **3**, pp. 4268–4278 (2011).
2. Dwivedi, N., Kumar, S., and Malik, H.K. "Superhard behaviour, low residual stress, and unique structure in diamond-like carbon films by simple bilayer approach", *Journal of Applied Physics*, **112**, p. 023518 (2012).
3. Nakazawa, H., Okuno, S., Magara, K., et al. "Tribological properties and thermal stability of hydrogenated, silicon/nitrogen-co incorporated diamond-like carbon films prepared by plasma-enhanced chemical vapor deposition", *Japanese Journal of Applied Physics*, **55**, 125501 (2016).
4. Robertson, J. "Diamond-like amorphous carbon", *Materials Science and Engineering: R: Reports*, **37**, pp. 129–281 (2002).
5. Li, H., Xu, T., Wang, C., et al. "Annealing effect on the structure, mechanical and tribological properties of hydrogenated diamond-like carbon films", *Thin Solid Films*, **515**, pp. 2153–2160 (2006).
6. Adhikary, S., Tian, X.M., Adhikari, S., et al. "Bonding defects and optical band gaps of DLC films deposited by microwave surface-wave plasma CVD", *Diamond and Related Materials*, **14**, pp. 1832–1834 (2005).
7. Ghadai, R.K., Das, S., Kumar, D., et al. "Correlation between structural and mechanical properties of silicon doped DLC thin films", *Diamond and Related Materials*, **82**, pp. 25–32 (2018).
8. Capote, G., Ramirez, M.A., Silva, P.C., et al. "Improvement of the properties and the adherence of DLC coatings deposited using a modified pulsed-DC PECVD technique and an additional cathode", *Surface and Coatings Technology*, **308**, pp. 70–79 (2016).
9. Ghadai, R.K., Kalita, K., Mondal, S.C., et al. "PECVD process parameter optimization: towards increased hardness of diamond-like carbon thin films", *Materials and Manufacturing Processes*, **33**(16), pp. 1905–1913 (2018).
10. Yang, Y. and Huang, W. "A grey-fuzzy Taguchi approach for optimizing multi-objective properties of zirconium-containing diamond-like carbon coatings", *Expert Systems with Applications*, **39**(1), pp. 743–750 (2012).
11. Singh, T.P. and Jatti, V.S. "Optimization of the deposition parameters of DLC coatings with the IC-PECVD method", *Particulate Science and Technology*, **33**(2), pp. 119–123 (2015).
12. Muthuraja, A., Naik, S., Rajak, D.K., et al. "Experimental investigation on chromium-diamond like carbon (Cr-DLC) coating through plasma enhanced chemical vapour deposition (PECVD) on the nozzle needle surface", *Diamond and Related Materials,* **100**, 107588 (2019).
13. Kilickap, E. "Modeling and optimization of burr height in drilling of Al-7075 using Taguchi method and response surface methodology", *The International Journal of Advanced Manufacturing Technology*, **49**, pp. 911–923 (2010).
14. Kilickap, E., Huseyinoglu, M., and Yardimeden, A. "Optimization of drilling parameters on surface roughness in drilling of AISI 1045 using response surface methodology and genetic algorithm", *The International Journal of Advanced Manufacturing Technology*, **52**, pp. 79–88 (2011).
15. Oliver, W.C. and Pharr, G.M. "An improved technique for determining hardness and elastic modulus using load and displacement sensing indentation experiments", *Journal of Materials Research*, **7**(6), pp. 1564–1583 (1992).
16. Ma, Y., Huang, X., Hang, W., et al. "Nanoindentation size effect on stochastic behavior of incipient plasticity in a $LiTaO_3$ single crystal", *Engineering Fracture Mechanics*, **226**, 106877 (2020).
17. Azadi Moghaddam, M., Golmezerji, R., and Kolahan, F. "Simultaneous optimization of joint edge geometry and process parameters in gas metal arc welding using integrated ANN-PSO approach", *Scientia Iranica*, **24**, pp. 260–273 (2017).
18. Hoa, T.N., Khatir, S., De Roeck, G., et al. "An efficient approach for model updating of a large-scale cable-stayed bridge using ambient vibration measurements combined with a hybrid metaheuristic search algorithm", *Smart Structures and Systems*, **25**, pp. 487–499 (2020).
19. Khatir, S., Khatir, T., Boutchicha, D., et al. "An efficient hybrid TLBO-PSO-ANN for fast damage identification in steel beam structures using IGA", *Smart Structures and Systems*, **25**, pp. 605–617 (2020).
20. Moghaddam, M.A. and Kolahan, F. "Modeling and optimization of the electrical discharge machining process based on a combined artificial neural network

and particle swarm optimization algorithm", *Scientia Iranica, Transaction B, Mechanical Engineering*, **27**, pp. 1206–1217 (2020).

21. Eberhart, R. and Kennedy, J. "A new optimizer using particle swarm theory", *Micro Machine and Human Science, 1995., MHS'95., Proceedings of the Sixth International Symposium on*, pp. 39–43 (1995).
22. Kalita, K., Ragavendran, U., Ramachandran, M., et al. "Weighted sum multi-objective optimization of skew composite laminates", *Structural Engineering and Mechanics*, **69**(1), pp. 21–31 (2019).
23. Tran-Ngoc, H., He, L., Reynders, E., et al. "An efficient approach to model updating for a multispan railway bridge using orthogonal diagonalization combined with improved particle swarm optimization", *Journal of Sound and Vibration*, **476**, 115315 (2020).
24. Tran-Ngoc, H., Khatir, S., Le-Xuan, T., et al. "A novel machine-learning based on the global search techniques using vectorized data for damage detection in structures", *International Journal of Engineering Science*, **157**, 103376 (2020).
25. Liu, W., Wang, Z., Zeng, N., et al. "A novel randomised particle swarm optimizer", *International Journal of Machine Learning and Cybernetics*, **12**(2), pp. 529–540 (2021).
26. Liao, Y., Zhang, L., and Li, W. "Regrouping particle swarm optimization based variable neural network for gearbox fault diagnosis", *Journal of Intelligent & Fuzzy Systems*, **34**(6), pp. 3671–3680 (2018).
27. Urfalioglu, O. "Robust estimation of camera rotation, translation and focal length at high outlier rates", *Computer and Robot Vision, 2004. Proceedings. First Canadian Conference on*, pp. 464–471 (2004).
28. Santos, C., Pinto, L., De Macedo Machado Freire, P., et al. "Application of a particle swarm optimization to a physically-based erosion model", *Annals of Warsaw University of Life Sciences-SGGW Land Reclamation*, **42**(1), pp. 39–49 (2010).
29. Santos, C., Freire, P.K., Mishra, S.K., et al. "Application of a particle swarm optimization to the tank model", *IAHS Publ*, **347**, pp. 114–120 (2011).
30. Kalita, K., Dey, P., Haldar, S., et al. "Optimizing frequencies of skew composite laminates with metaheuristic algorithms", *Engineering with Computers*, **36**(2), pp. 741–761 (2020).
31. Ghadai, R.K., Das, S., Kalita, K., et al. "Effect of nitrogen (N2) flow rate over the tribological, structural and mechanical properties diamond-like carbon (DLC) thin film", *Materials Chemistry and Physics*, **260**, 124082 (2021).
32. Ghadai, R.K., Das, S., Kalita, K., et al. "Structural and mechanical analysis of APCVD deposited diamond-like carbon thin films", *Silicon*, **13**, pp. 4453–4462 (2020).
33. Das, S., Guha, S., Das, P.P., et al. "Analysis of morphological, microstructural, electrochemical and nano mechanical characteristics of TiCN coatings prepared under N2 gas flow rate by chemical vapour deposition (CVD) process at higher temperature", *Ceramics International*, **46**(8), pp. 10292–10298 (2020).

Biographies

Kanak Kalita is an Assistant Professor at Vel Tech Rangarajan Dr Sagunthala R&D Institute of Science and Technology, Avadi, India. He received his BSc degree in mechanical engineering from RGTU, Bhopal, India; MSc and PhD in Aerospace Engineering and Applied Mechanics from the Indian Institute of Engineering, Science & Technology, Shibpur, India. He is the Associate Editor of 2 Scopus journals and has reviewed 300+ manuscripts for 60+ journals and conferences. He has been awarded thrice by Publons for his reviewing efforts. He has published 56 SCI and 91 Scopus research articles and edited 3 book volumes for IOP publishers, Springer, and AIP publications. His areas of interest include machine learning based metamodeling, process optimization, finite element method, and composites.

Ranjan Kumar Ghadai received his B. Tech in mechanical engineering from Biju Patnaik University of technology, Odissa, India followed by MSc and PhD in mechanical engineering from the Indian Institute of Engineering, Science & Technology, Shibpur, India. He is currently an Assistant Professor in the Department of Mechanical Engineering at Sikkim Manipal Institute of Technology, India. He has published 40+ SCI/SCOPUS research articles and edited 3 book volumes for IOP publishers, Springer, and AIP publications. His research interests include thin-film coatings, experimental non-traditional machining, and optimization of machining processes.